Asymmetric nuclear motion of the F 1*s*−ionized state in BF_3 probed by quadruple-ion-coincidence momentum imaging

A. De Fanis,[1,2] N. Saito,[3] M. Machida,[4] K. Okada,[5] H. Chiba,[1] A. Cassimi,[6] R. Dörner,[7] I. Koyano,[4] and K. Ueda[1,*]

[1]*Institute of Multidisciplinary Research for Advanced Materials, Tohoku University, Sendai 980-8577, Japan*

[2]*Japan Synchrotron Radiation Research Institute, Sayo-gun, Hyogo 679-5198, Japan*

[3]*National Metrology Institute of Japan, AIST, Tsukuba 305-8568, Japan*

[4]*Department of Material Science, Himeji Institute of Technology, Kamigori 678-1297, Japan*

[5]*Department of Physical Science, Hiroshima University, Higashi-Hiroshima 739-8526, Japan*

[6]*CIRIL/CEA/CNRS/ISMRA, Université de Caen, Box 5133, F-14070 Caen Cedex 5, France*

[7]*Institut für Kernphysik, University of Frankfurt, August Euler Straße 6, D-60486 Frankfurt, Germany*

(Received 18 July 2003; published 18 February 2004)

Using the quadruple-ion-coincidence momentum imaging technique, we find that the momentum correlation of the four atomic ions departed from one BF_3^{4+} parent molecular ion produced via multiple Auger decay after F 1*s* ionization exhibits asymmetric fragmentation in which the B^+ ion is ejected in the direction opposite to one of the F^+ ions. This observation provides evidence of symmetry lowering, from D_{3h} to C_{3v} in the F 1*s*−ionized state.

DOI: 10.1103/PhysRevA.69.022506 PACS number(s): 33.15.Bh, 33.20.Wr, 33.20.Rm

I. INTRODUCTION

Essential properties of molecules depend critically on the conformation and its symmetry. Consequently, changes in the conformation lead to new properties. A great body of research exists on molecular conformation and its deformation by photon excitation [1].

Core excitation is a very effective way to induce molecular deformation. This is because the stable conformation of the core-excited state is generally different from that of the ground state. This deformation breaks the symmetry of the molecule and affects subsequent electronic decay and ionic fragmentation: sometimes it opens a new fragmentation channel [2,3]. Typical examples for the molecular deformation initiated by the promotion of the core electron to the lowest unoccupied molecular orbital (LUMO) may be seen in the C 1*s* excitation of the linear molecule CO_2 in the $D_{\infty h}$ point group [3–6], as well as in the B 1*s* excitation of the plane molecule BF_3 in the D_{3h} point group [7–11]. In the former case, the twofold Π_u state in which the C 1*s* electron is promoted to LUMO splits into two due to Renner-Teller effects and the lower branch of the Renner-Teller state becomes stable in the C_{2v} bent conformation (see, for example, Ref. [6]). In the latter case, the A_2'' state in which the B 1*s* electron is promoted to LUMO becomes stable in the C_{3v} pyramidal conformation due to pseudo-Jahn-Teller couplings (see, for example, Ref. [10]). The molecular deformations initiated by the promotion of the core electron to LUMO were probed via angle-resolved ion yield study [4,6,8], coincidence study [3,5,7,8], and resonant photoemission study [3,9,11].

Core excitation or ionization of the equivalent atoms in a symmetric molecule forms another class of symmetry lowering in the core-excited or ionized states. In this case, asymmetric vibrations arise due to vibronic couplings, i.e., pseudo-Jahn-Teller mixing among the nearly degenerate core-excited or ionized states and reflect symmetry lowering. A well-known example in this class may be the O 1*s* photoionization of CO_2 [12–14]. When one O 1*s* electron is ionized, the potentials at the oxygen atoms are no longer identical and thus the O 1*s*−ionized molecule has a new stable conformation where the C–O bond lengths differ. The excitation of the antisymmetric stretching vibrations in the O 1*s*−ionized state of CO_2, which is forbidden in the absence of the vibronic coupling, was predicted by Domcke and Cederbaum in 1977 and observed by Kivimäki *et al.* 20 years later. More recently, Ueda *et al.* observed symmetry lowering from T_d to C_{3v} in the F 1*s*−excited states of a symmetric molecule CF_4 [15]: they found the Doppler energy shift of the F atomiclike Auger emission, when they measured the resonant photoemission from CF_4 in the direction parallel to the electric vector, as direct evidence that the ultrafast F^*-CF_3 dissociation along the electric vector of the incident light is caused in the F 1*s*−excited state, where F* indicates 1*s*-excited F atom.

In the present paper, we focus on symmetry lowering of the F 1*s*−ionized state of the BF_3 molecule. Here one could expect that asymmetric nuclear motion of e' symmetry arises due to vibronic coupling, i.e., pseudo-Jahn-Teller mixing among the nearly degenerate F 1*s*−ionized states, and thus the molecular symmetry is lowered from D_{3h} to C_{2v}, reflecting dynamical core-hole localization. The aim of the present work is to probe this asymmetric nuclear motion, which has never been detected. The angular distribution measurements of the fragment ions, which have been used to probe molecular deformation of CO_2 and BF_3 due to promotion of the core electron of the central atom (C or B) to LUMO [4,6,8], was insensitive to the molecular deformation from D_{3h} to C_{2v} [16]. Core-level photoelectron spectroscopy, which has been successfully applied to O 1*s* photoemission from CO_2 [13], did not work: no vibrations were

*Electronic address: ueda@tagen.tohoku.ac.jp

observed in the F $1s$ photoelectron spectrum with the total experimental resolving width of less than 100 meV [17]. This may be because the vibrational structure in the F $1s$ photoelectron is complex due to multimode couplings and is not resolved owing to the lifetime width of the F $1s$–ionized state of about 200 meV. The Doppler energy shift in the Auger emission from the F fragment, detected in the resonant photoemission from CF_4 [15], could not be observed, implying that F $1s$–ionized BF_3 does not experience ultrafast dissociation [17].

The alternative method we employ here is the quadruple-ion-coincidence momentum imaging technique. This technique is based on the time-of-flight (TOF) method combined with a two-dimensional [2D, i.e., (x,y)] position-sensitive detector. Using this three-dimensional [3D, i.e., (x,y,t)] TOF spectrometer, we detect all the four fragment ions produced from the quadruply charged parent ions $BF_3{}^{4+}$. Registration of all the ions in coincidence allows us to extract all the kinematical information for the linear momentum (P_x,P_y,P_z) of each fragment ion without ambiguity. The quadruply charged $BF_3{}^{4+}$ molecular parent ion can be produced by the multiple Auger decay of the F $1s$–ionized state of BF_3. This channel is very weak, representing less than 1% of the total ionization yield. This quadruply charged molecular ion has high internal energy and breaks up very rapidly due to Coulomb explosion. Thus, despite the small branching ratio for the formation of the quadruply charged $BF_3{}^{4+}$ molecular parent ion, the vector correlation among the linear momenta of the four ions reflects the conformation of the F $1s$–ionized BF_3 at the time when the Auger decay takes place, because the properties of the excited state are independent of the decay channels. We have tested this technique to detect the well-known deformation from D_{3h} to C_{3v} due to promotion of the B $1s$ electron to LUMO [18]: the results were consistent with observations by other techniques [7–11,18] and theoretical predictions [7,10].

II. EXPERIMENT

The experiment has been performed at the *c* branch of the soft x-ray photochemistry beamline 27SU at SPring-8 [19,20]. The light source is a figure-8 undulator and provides linearly polarized light [21]. The measurements have been carried out with multiple-ion-coincidence momentum imaging apparatus. Briefly, a skimmed supersonic gas jet intersects the radiation beam at 90°; charged particles are accelerated by a uniform electrostatic field of ~20 V/mm along the axis of the 3D-TOF perpendicular to the gas and photon beams. The length of the acceleration region is ~70 mm. Ions are detected by a multichannel plate (MCP) at the end of a field-free TOF tube 140 mm long, coupled with a three-layer hexagonal delay line anode with the effective diameter of 80 mm (HEX80 manufactured by Roentdek) that allows us to extract the two-dimensional position coordinate and arrival time (x,y,t), even for the coincidence detection of the three F^+ fragments with the same mass. Electrons are detected by a different MCP placed at the opposite end of the accelerating region. The detection of the electrons gives the origin of the TOF measurement for ions.

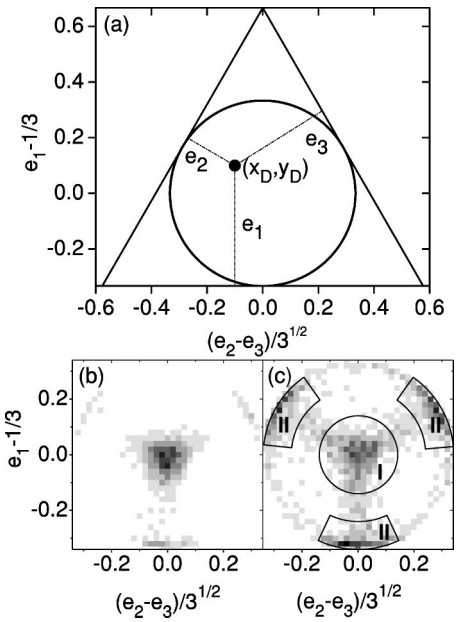

FIG. 1. (a) Definition of the axis for the construction of the Dalitz diagrams. Dalitz plots constructed with the projection of the $F_i{}^+$ momenta to the plane perpendicular to the emission of B^+, the indices *i* are randomly assigned. (b) and (c), events recorded on top of the B and F $1s\rightarrow 4e'$ shape resonances, respectively. See text for further details.

III. RESULTS AND DISCUSSION

The vector correlation among the linear momenta of three particles produced by the three-body breakup can be well represented by the Dalitz plots [22]. Figure 1(a) helps to explain the way to construct the Dalitz plot. We introduce the normalized, squared momentum e_i for each ion *i*,

$$e_i=\frac{|P_i|^2}{\Sigma_i|P_i|^2}, \tag{1}$$

where P_i is the linear momentum of the ion *i*, and define the Cartesian coordinates x_D and y_D as

$$x_D=\frac{e_2-e_3}{3^{1/2}},\ y_D=e_1-\tfrac{1}{3}. \tag{2}$$

Then all the data points (x_D,y_D) are within the circle in Fig. 1(a) and the distances from the data point (x_D,y_D) to the three sides of the regular triangle are e_i.

We construct Dalitz plots with the projection of the linear momenta of the three F^+ ions to the plane perpendicular to the linear momentum of B^+; these projections are called p_i here. In Figs. 1(b) and (c), we compare the Dalitz plots thus constructed for the B $1s$ ionization and F $1s$ ionization of BF_3. In both cases, the photon energies were tuned to the peak of the shape resonance, designated as $4e'$, in order to obtain the maximum count rates. For the construction of the plots in Figs. 1(b) and (c), the indexes $i=1$, 2, 3 labeling the three F^+ ions are randomly assigned.

The B $1s$–ionized state is known to have the D_{3h} equilibrium conformation [7] and thus does not manifest symmetry

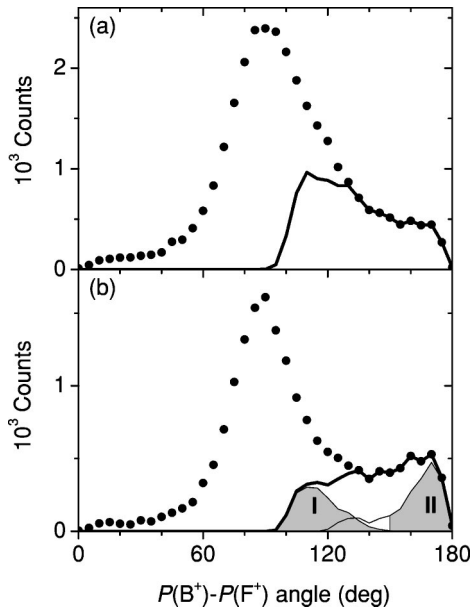

FIG. 2. Distributions of correlation angles between $P(B^+)$ and $P(F^+)$ recorded on top of the (a) B and (b) F $1s \rightarrow 4e'$ shape resonances. Points, F^+ is randomly picked; thick line, F^+ is the one ejected closest to the direction opposite to $P(B^+)$; thin line, events gated by the masked areas I and II in Fig. 1.

lowering. We present Fig. 1(b) as a reference for comparison. This plot confirms that $|p_i|^2$ of the projected linear momenta of the three F^+ ions are almost the same and thus the threefold axial symmetry along the linear momentum of B^+ is kept in the four-body breakup. In the plot of Fig. 1(c) for the F 1s ionization, we find that considerable amount of the data points appear along one of the three ternary axis closer to one side of the triangle. These events correspond to the momentum sharing in which the projection for one of the three F^+ to the plane perpendicular to the B^+ ejection is almost zero. One can imagine that these events reflect asymmetric stretching nuclear motion in the F 1s−ionized state. We will demonstrate that it is really the case. The masked areas I and II in Fig. 1(c) will be used later to gate symmetric and asymmetric events, respectively.

In Figs. 2(a) and (b), we present the distributions of the correlation angles between the linear momentum of B^+, $P(B^+)$, and randomly selected of F^+, $P(F_i{}^+)$, for the B 1s and F 1s ionizations, respectively. We notice that the distribution of the correlation angles displays an asymmetry with a larger yield at angles larger than 90° and this asymmetric contribution increases for the F 1s ionization. The small peak at about 170° which appears in the distribution for the F 1s ionization [Fig. 2(b)] corresponds to the breakup in which B^+ and one of F^+ fly apart in opposite directions. In order to select such events, we label F^+ that goes to the direction closest to the direction opposite to $P(B^+)$ as $F_a{}^+$ and the other two as $F_b{}^+$ and $F_c{}^+$. The distribution of the correlation angle between $P(F_a{}^+)$ and $P(B^+)$ is also displayed in Fig. 2(b) (thick line). Figure 2(b) also contains the distributions of the correlation angle between $P(F_a{}^+)$ and $P(B^+)$ for the I and II selection from Fig. 1(c). By comparing the distributions of angles for the I and II selection we find out that the

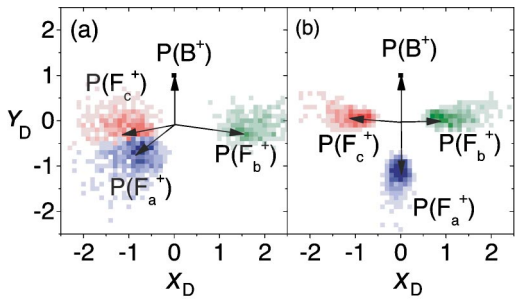

FIG. 3. Newton diagrams for the symmetric (a) and asymmetric (b) events, respectively. Here the F^+ that goes to the direction closest to the opposite to $P(B^+)$ is labeled as $F_a{}^+$ and the other two as $F_b{}^+$ and $F_c{}^+$. The diagrams are constructed for the momenta projected to the plane defined by $P(B^+)$ and $P(F_b{}^+)$. See text for further details.

data points closer to one side of the triangle correspond to the events in which B^+ and $F_a{}^+$ fly apart in opposite directions. The smaller structure in the distribution for the II selection that peaks near 130° corresponds to the events in which one of F^+ receives recoil momentum of nearly zero and thus may be considered as sequential decay.

In order to illustrate how the four ions fly apart, we employ here Newton diagrams. Newton diagrams are conventionally used to display correlations of three linear momenta for the three-body breakup. To display correlations of four linear momenta for the four-body breakup, we define the plane by $P(B^+)$ and $P(F_b{}^+)$ and take the projections of $P(F_a{}^+)$ and $P(F_c{}^+)$ to this plane. Then the amplitudes of the four momenta within this plane are normalized in such a way that the amplitude of $P(B^+)$ is unity. Figures 3(a) and (b) correspond to the Newton diagrams thus produced for the symmetric and asymmetric events falling in the masked areas I and II in Fig. 1(c), respectively. The data in Fig. 3(b) are further selected by requiring the angle between $P(F_a{}^+)$ and $P(B^+)$ to be larger than 150°. Here the unit vector corresponding to the normalized $P(B^+)$ is set to the positive y direction, $(x,y)=(0,1)$.

From Figs. 2(b) and 3(a), it is clear that the symmetric events I are the breakup within the threefold symmetry, where B^+ is ejected perpendicularly to the molecular plane and three F^+ are ejected nearly within the molecular plane. This breakup pattern reflects that the four-body breakup of $BF_3{}^{4+}$ by the Coulomb explosion starts at the conformation close to the ground state of D_{3h} symmetry. The reason why B^+ is ejected perpendicularly to the molecular plane may be due to zero-point out-of-plane vibration; this zero-point vibration can be enhanced significantly by the Coulomb repulsion from the three F^+ ions.

Figure 3(b), on the other hand, clearly illustrates that the asymmetric events (II) are the breakup within the molecular plane, where B^+ and $F_a{}^+$ fly apart in opposite directions and $F_b{}^+$ and $F_c{}^+$ fly apart in opposite directions perpendicular to B^+ and $F_a{}^+$. This can happen only when the four-body breakup by the Coulomb explosion starts at the conformation in which the central B atom is off center in the direction of one B–F bond. Thus the enhancement of the asymmetric events (II) by the F 1s ionization is direct proof that asym-

metric nuclear motion, which brings the central B atom off center within the molecular plane, is initiated by the F $1s$ ionization. Note that the multiple Auger decay may take place before the central B atom sufficiently moves, even though the asymmetric nuclear motion is initiated in the F $1s$–ionized state. Then four-body break-up by the Coulomb explosion ends up with the symmetric events I. Note also that the asymmetric events take place for the B $1s$ ionization as well [see Figs. 1(b) and 2(a)] due to the zero-point asymmetric vibration, though the amount is far less than that for the F $1s$ ionization.

Finally we note the correlation between the symmetry-lowering axis and the polarization axis. The asymmetry parameters β of B^+ and F^+ for the symmetric four-body breakup events I are -0.4 ± 0.1 and 0.4 ± 0.1, respectively. These β values suggest that the F^+ (B^+) is ejected preferentially within (perpendicularly to) the molecular plane whose plane normal is preferentially oriented perpendicularly to the polarization vector due to e' character of the shape resonance. The β parameters of B^+ and $F_a{}^+$ for the asymmetric events (II) are 0.7 ± 0.1. These strongly positive values illustrate that B^+ and $F_a{}^+$ are emitted preferentially along the polarization vector and thus the direct evidence that the elongation of the B–F bond due to asymmetric nuclear motion resulting in the $D_{3h}\rightarrow C_{2v}$ symmetry lowering takes place preferentially along the polarization vector.

In conclusion, we have observed that F $1s$ ionization of the D_{3h} plane molecule enhances the four-body breakup in which B^+ and one of F^+ fly apart in opposite directions and the other two F^+ fly apart in opposite directions perpendicular to the B^+-F^+ breakup and that the B^+-F^+ breakup axis is preferentially oriented to the polarization vector. This breakup directly reflects the asymmetric nuclear motion, along the polarization vector, in the F $1s$–ionized state. This asymmetric nuclear motion has never been observed by any other techniques. The quadruple-ion-coincidence momentum imaging technique made this observation possible.

ACKNOWLEDGMENTS

This experiment was carried out with the approval of the SPring-8 program advisory committee. We are grateful to the staff at SPring-8 for their help, and to A. Czasch for help with the multihit encoding. This work was supported in part by Grants-in-Aid for Scientific Research from the Japan Society for the Promotion of Science (JSPS). A.D. is grateful to JSPS for financial support during his stay at Tohoku University. R.D. acknowledge financial support by DFG and BMBF.

[1] G. Herzberg, *Molecular Spectra and Molecular Structure, II, III* (Van Nostrand Reinhold, New York, 1966).
[2] K. Ueda, M. Simon, C. Miron, N. Leclercq, R. Guillemin, P. Morin, and S. Tanaka, Phys. Rev. Lett. **83**, 3800 (1999).
[3] P. Morin, M. Simon, C. Miron, N. Leclercq, E. Kukk, J. D. Bozek, and N. Berrah, Phys. Rev. A **61**, 050701 (2000).
[4] J. Adachi, N. Kosugi, E. Shigemasa, and A. Yagishita, J. Chem. Phys. **107**, 4919 (1997).
[5] Y. Muramatsu, K. Ueda, N. Saito, H. Chiba, M. Lavollée, A. Czasch, Th. Weber, O. Jagutzki, H. Schmidt-Böcking, R. Moshammer, U. Becker, K. Kubozuka, and I. Koyano, Phys. Rev. Lett. **88**, 133002 (2002).
[6] H. Yoshida, K. Nobusada, K. Okada, S. Tanimoto, N. Saito, A. De Fanis, and K. Ueda, Phys. Rev. Lett. **88**, 083001 (2002).
[7] M. Simon, P. Morin, P. Lablanquie, M. Lavollée, K. Ueda, and N. Kosugi, Chem. Phys. Lett. **238**, 42 (1995).
[8] K. Ueda, K. Ohmori, M. Okunishi, H. Chiba, Y. Shimizu, Y. Sato, T. Hayaishi, E. Shigemasa, and A. Yagishita, Phys. Rev. A **52**, R1815 (1995).
[9] M. Simon, C. Miron, N. Leclercq, P. Morin, K. Ueda, Y. Sato, S. Tanaka, and Y. Kayanuma, Phys. Rev. Lett. **79**, 3857 (1997).
[10] S. Tanaka, Y. Kayanuma, and K. Ueda, Phys. Rev. A **57**, 3437 (1998).
[11] C. Miron, R. Feifel, O. Börneholm, S. Svensson, A. Naves de Brito, S. L. Sorencen, M. N. Piancastelli, M. Simon, and P. Morin, Chem. Phys. Lett. **359**, 48 (2002).
[12] W. Domcke and L. S. Cederbaum, Chem. Phys. **25**, 189 (1977).
[13] A. Kivimäki, B. Kempgens, K. Maier, H. M. Köppe, M. N. Piancastelli, M. Neeb, and A. M. Bradshaw, Phys. Rev. Lett. **79**, 998 (1997).
[14] N. V. Dobrodey, H. Köppel, and L. S. Cederbaum, Phys. Rev. A **60**, 1988 (1999).
[15] K. Ueda, M. Kitajima, A. De Fanis, T. Furuta, H. Shindo, H. Tanaka, K. Okada, R. Feifel, S. L. Sorensen, H. Yoshida, and Y. Senba, Phys. Rev. Lett. **90**, 233006 (2003).
[16] Y. Shimizu, K. Ueda, H. Chiba, M. Okunishi, K. Ohmori, J. B. West, Y. Sato, and T. Hayaishi, J. Chem. Phys. **107**, 2419 (1997).
[17] K. Ueda, A. De Fanis, M. Kitajima *et al.* (unpublished).
[18] K. Ueda, A. De Fanis, N. Saito, M. Machida, K. Kubozuka, H. Chiba, Y. Muramatsu, Y. Sato, A. Czasch, O. Jaguzki, R. Dörner, A. Cassimi, M. Kitajima, T. Furuta, H. Tanaka, S. L. Sorensen, K. Okada, S. Tanimoto, K. Ikejiri, Y. Tamenori, H. Ohashi, and I. Koyano, Chem. Phys. **289**, 135 (2003).
[19] H. Ohashi, E. Ishiguro, Y. Tamenori, H. Kishimoto, M. Tanaka, M. Irie, and T. Ishikawa, Nucl. Instrum. Methods Phys. Res. A **467-468**, 529 (2001).
[20] H. Ohashi, E. Ishiguro, Y. Tamenori, H. Okumura, A. Hiraya, H. Yoshida, Y. Senba, K. Okada, N. Saito, I. H. Suzuki, K. Ueda, T. Ibuki, S. Nagaoka, I. Koyano, and T. Ishikawa, Nucl. Instrum. Methods Phys. Res. A **467-468**, 533 (2001).
[21] T. Tanaka and H. Kitamura, J. Synchrotron Radiat. **3**, 47 (1996).
[22] R. H. Dalitz, Philos. Mag. **44**, 1068 (1953).